ISSN 1063-7842, Technical Physics, 2020, Vol. 65, No. 11, pp. 1771–1776. © Pleiades Publishing, Ltd., 2020.
Russian Text © The Author(s), 2020, published in Zhurnal Tekhnicheskoi Fiziki, 2020, Vol. 90, No. 11, pp. 1854–1859.

PHYSICAL SCIENCE OF MATERIALS

Morphology and Structure of Defected Niobium Oxide Nonuniform Arrays Formed by Anodizing Bilayer Al/Nb Systems

A. Pligovka[a,*], P. Yunin[b], A. Hoha[a], S. Korolyov[b], G. Gorokh[a], and E. Skorokhodov[b]

[a] *Research and Development Laboratory 4.10 "Nanotechnologies," Belarusian State University of Informatics and Radioelectronics, Minsk, 220013 The Republic of Belarus*

[b] *Institute for Physics of Microstructures, Russian Academy of Sciences, Nizhny Novgorod, 603087 Russia*

**e-mail: pligovka@bsuir.by*

Received April 28, 2020; revised April 28, 2020; accepted April 28, 2020

Abstract—The work is devoted to the X-ray diffraction research of defected niobium oxide nonuniform (NON) arrays and niobium oxide nanocolumns formed by electrochemical anodizing. The obtained results allow to make an assumption about the probable presence of a significant amount of NbO, $NbO_{0.7}$, Nb_2O_5 and a small amount of NbO_2, and Al in the composition of defected NON and the presence of all these substances in the nanocolumns of niobium oxide except $NbO_{0.7}$, but in smaller quantities. The comparative analysis of the NON structure and the nanocolumns makes it possible to isolate, probably, a significant amount of $Nb_{0.94}O_{0.06}$, Nb_6O in the defected nanocolumns, which was not found in NON.

DOI: 10.1134/S1063784220110213

INTRODUCTION

The research of electrochemical anodic oxidation (anodizing) processes of valve metals through anodic aluminum oxide (AAO) pores is very relevant, since anodizing allows creating arrays of uniformly hexagonal close-packed nanostructured oxide nonuniform arrays, whose morphology, composition and physical properties can be controlled by changing the anodizing modes [1–5]. Reanodizing of such nonuniform arrays leads to the formation of full niobium oxide nanocolumns [6]. Similar arrays of nanocolumns can also be formed from the anodic oxide of tantalum, hafnium and tungsten [7–9]. The investigations have shown [10] that niobium oxide nonuniformities (NON) have different morphology, in contrast, for example, to the nonuniformities of tantalum oxide, which have the same spherical shape in all previously established anodizing modes [2]. From the work [11] it can be observed that the NONs differ not only in size, but also in the shape and the nature of their arrangement. The main works [2, 6] on this topic are devoted to the research of the morphology and composition of niobium oxide nanocolumns, while the composition of the NON themselves is little investigated. The results of the NON research by X-ray photoelectron spectroscopy (XPS) are presented in [11]. The NON was formed by anodizing in 0.8 M aqueous tartaric acid solution at a forming voltage 200 V. The shape of such NON was cup-shaped, which is typical for this mode [10]. The research showed the presence of Nb, O, Al, and C in the composition of the investigated formations. Deep profiling was determined by the peaks of Nb 3*d*, Al 2*p*, O 1*s*, and C 1*s*. The carbon peak disappeared immediately after the beginning of Ar^+ sputtering, indicating that carbon-containing particles were not included in the NON. At the beginning of Ar^+ sputtering, the measured Nb 3*d* spectrum consisted of a double peak ($3d_{5/2}$ and $3d_{3/2}$) corresponding to the Nb^{5+} state. In 3 min, a shoulder appeared at the low-energy edge of the Nb_2O_5 peak, which then developed into an additional double peak with binding energies of 201.5 and 204.3 eV, which are typical binding energies for $3d_{5/2}$ and $3d_{3/2}$ electrons in the Nb^0 state. During sputtering, the position of the niobium metal peak remained virtually unchanged, and its intensity increased, reaching its maximum when the sputtering time exceeded 100 min. The two peaks existed simultaneously until the peak of niobium V oxide became vague (10 min); however, the shoulder at the high energy boundary of the peak of metallic niobium remained for 20 min of Ar^+ sputtering. This indicates a transition from stoichiometric Nb_2O_5 on the surface to metallic niobium with the simultaneous existence of both metal and niobium V oxide during sputtering. The described evolution of the two peaks also suggested the presence of niobium suboxides in the film. In addition, the appearance and evolution of the niobium metal peak suggested the presence of non-oxidized niobium metal around the NON bottoms. The relatively slow increase in the intensity of the Nb^0 peak at the beginning of Ar^+ sputtering could be explained by the coating of the niobium film with

residual aluminum, which was simultaneously sputtered by the Ar^+ beam. The initial sputtering spectrum consisted of two different symmetrical peaks: the first is at 72.2 eV, associated with the Al^0 state (higher intensity), and the second is at 74.8 eV (lower intensity), which refers to the Al^{3+} state. After the first sputtering cycle, the intensity of both peaks increased to the same degree, but then the pair began to be dominated by the peak Al^0. The peak of Al^{3+} abruptly decreased and completely disappeared after 20 min of sputtering. Conversely, the peak of metallic aluminum increased with the time of sputtering and after reaching the maximum gradually decreased, however, not disappearing completely within 180 min after sputtering Ar^+. It is obvious that the strong and long profiled peak of Al^0 is due to the large amount of metallic aluminum surrounding the NON. The relatively short depth profile for the Al^{3+} peak implies that the aluminum oxide was located only in the outer part of the NON (most likely in the tops—Fig. 1). The measured O 1*s* spectrum of the sample not treated with Ar^+ consisted of a symmetrical peak with an energy 531.8 eV, which could be associated with oxygen bound in the AAO. During Ar^+ sputtering, the position of the O 1*s* peak gradually shifted towards lower energies, and after 18 min, the peak was registered at 530.7 eV, which characterized this peak as corresponding to the oxygen bound in niobium oxide. This corresponds well to the depth profile of the Al^{3+} peak identified as part of the NON, and confirms the assumption of the external location of aluminum in the structure of the NON top. Thus, the analysis of the literature data allows to assess the NON surface composition, but the literature sources did not give information about the NON internal composition. Such researches can be carried out by using simultaneously two methods: breaking the NON integrity, defected them on the one hand, and applying the research X-ray diffraction method [12] on the other.

The purpose of this work was to investigate the composition of mechanically defected arrays of niobium oxide nonuniformities formed by electrochemical anodizing of a two-layer Al/Nb system using X-ray phase analysis (XPA) [13, 14].

EXPERIMENTAL

The process of forming the NON system is shown in Fig. 1. The initial samples were 100 mm Si wafers (*n*-type, 4 Ω cm), on which two-layer Al/Nb systems (1500/300 nm) were applied by magnetron-sputtering, as shown in Fig. 1a. Prior to the anodizing process, the Si wafer was cut into samples with an area of 3×3 cm^2. The anodizing process itself was performed in a cylindrical two-electrode cell made of polytetrafluoroethylene (PTFE). The anodizing cell consisted of an electrolytic bath with a built in anode that pressed a sample of the Si wafer with magnetron-sputtering metals (an experimental sample) to the cell base, thereby eliminating the meniscus effect and parasitic oxidation of the Si wafer. The cathode, located in the electrolyte, was made of stainless steel. The experimental sample was individually placed in an anode cell and pressed against the aluminum side by a PTFE ring, so that a circular area of 2.83 cm^2 could be in contact with the anodizing solution, while the reverse Si wafer side was completely isolated from the electrolyte. At the first stage, aluminum was anodized until it was completely acidified, as shown in Fig. 1b, in 0.4 M H_3PO_4 aqueous solution at a voltage 100 V. Anodizing was carried out in a potentiostatic mode, the achievement of the niobium sublayer by the AAO barrier layer was indicated by the beginning of a current drop at the kinetic dependence. At the next stage, during a smooth drop of the anode current, the process of anodizing the niobium sublayer through the AAO pores to the NON formation, as shown in Fig. 1c. To conduct a composition comparative analysis, niobium anodic oxide nanocolumns were formed in 0.4 M $C_2H_2O_4$ aqueous solution at a voltage 37 V, followed by high-voltage reanodizing to a voltage 190 V in a solution of 0.5 M H_3BO_3 and 0.05 M $Na_2B_4O_7$, as shown in Fig. 1e. Nanocolumns formation process of this type is described thoroughly in [6]. The anodizing modes were set using a Keysight N5752A power supply, and the parameters were registered and monitored in situ using a Keysight 34470A. During the anodizing process, the room temperature (23°C) was maintained with an accuracy of ±1°C. The porous AAO was removed in 50% aqueous solution of H_3PO_4 at 50°C for 30 min.

The morphology was researched using scanning electron microscopy (SEM) using a Carl Zeiss Supra 50VP electron microscope. The phase composition was researched using a Bruker D8 Discover X-ray diffractometer. The analysis was performed by theta–2 teta scanning using a position-sensitive detector LYNXEYE, radiation—CuK_α.

X-ray analysis methods are widely used to research the structure, composition and properties of various materials. The widespread of XPA is facilitated by its objectivity, versatility, speed of many of its methods, accuracy and the ability to solve a variety of problems that are often not available for other research methods. With the help of XPA one can investigate: qualitative and quantitative mineralogical and phase composition of materials, as the only method for controlling the phase composition. XPA is based on the fact that each crystal phase gives an individual, unique picture of the diffraction maxima location and their intensities [15–18]. To investigate the internal composition of NONs and nanocolumns, mechanical flaw detection and targeted partial destruction of nanostructures were performed to ensure guaranteed access of detecting radiation to their internal structure (Figs. 1d, 1f). To a certain extent, this technique was probably

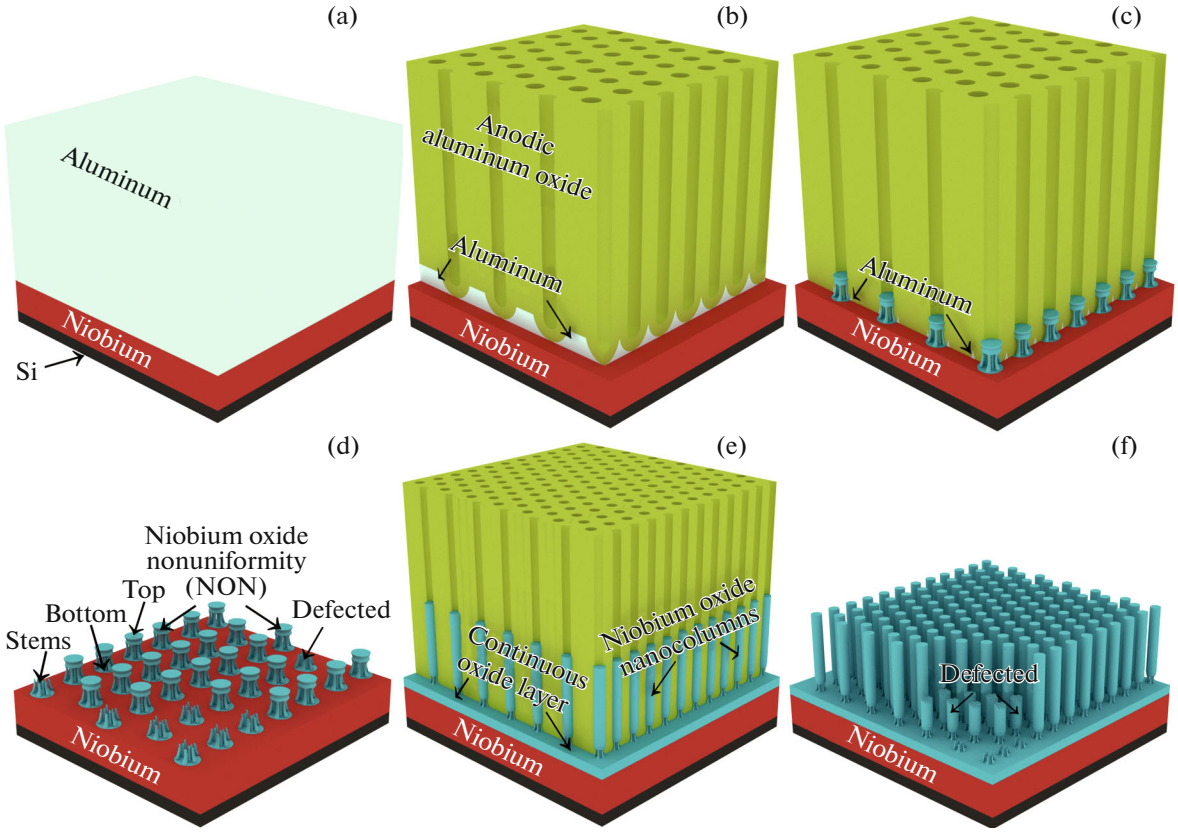

Fig. 1. The schematic 3D view shows the main stages of forming niobium oxide nonuniform (NON) arrays and nanocolumns by anodizing of a two-layer Al/Nb system on a Si wafer: (a) sputter-deposited of a two-layer Al/Nb system on a Si wafer; (b) Al anodizing to form a porous anodic aluminum oxide (AAO); (c) anodizing of the Nb sublayer through AAO pores; (d) removal of porous AAO by chemical etching and mechanical defected of NON; (e) higher-voltage reanodizing of the Nb sublayer through the AAO pores; (f) removal of porous AAO by chemical etching and mechanical defecting process of niobium oxide nanocolumns. (c) NON formed by anodizing in 0.4 M H_3PO_4 aqueous solution at a voltage 100 V; (f) niobium oxide nanocolumns formed by anodizing in 0.4 M $C_2H_2O_4$ aqueous solution at a voltage 37 V and reanodized in 0.5 M H_3BO_3 aqueous solution and 0.05 M $Na_2B_4O_7$ to a voltage 190 V.

redundant, since X-ray radiation has a high penetrating power. These circumstances led to the use of a research method based on X-ray diffraction [19], which allows reliable, simple, inexpensive and affordable way to analyze NONs-samples, obtaining an integral picture of their phase composition to a great depth [14].

RESULTS AND DISCUSSION

Figure 2a shows the SEM image of the surface of NONs formed in 0.4 M H_3PO_4 aqueous solution at a voltage 100 V and with a removed porous AAO. Figure 2a shows that the entire surface is uniformly covered with mechanically defected NONs of the same shape, size, and frequency. All NONs consist of the bottom located in the Nb film, the top located in the AAO pore before its removal, and the stems connecting the bottom and the top located in the AAO barrier layer before its removal. The described NONs have unique morphological features that distinguish them from other types of NONs presented in [11, 12]: the first, the NON stems are located at a significant equidistant distance from each other; the second, the NON diameter is commensurate with their height. Research conducted earlier shows [10, 11] that all other known conditions of formation do not allow to obtain NON with such morphological features.

Figure 2b shows the SEM image of the surface at an angle of niobium oxide nanocolumns formed in 0.4 M $C_2H_2O_4$ aqueous solution at a voltage 37 V and then reanodizing to a voltage 190 V in an aqueous solution of 0.5 M H_3BO_3 and 0.05 M $Na_2B_4O_7$. Before SEM observations, the porous AAO was removed. Figure 2b shows that the entire surface is uniformly covered with mechanically defected nanocolumns of the same shape and size. The shape of the nanocolumns fully corresponds to the one described earlier in [6].

Figure 3a shows the results of the XPA of defected NONs. Previously, the complete removal of the porous AAO was performed. Investigations have shown the presence of one strong peak near 36°, which

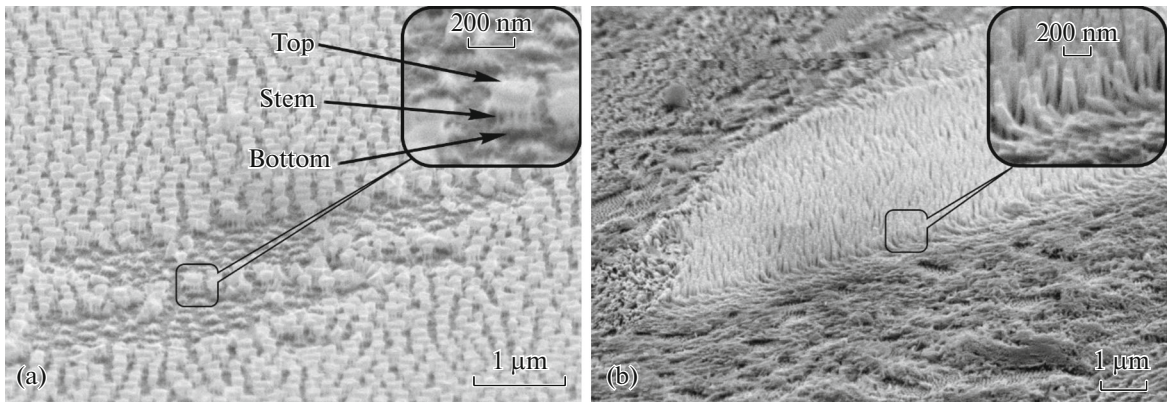

Fig. 2. Scanning electron microscopy of defected niobium oxide nonuniform (NON) arrays formed by anodizing a two-layer Al/Nb system in 0.4 M H_3PO_4 aqueous solution at a voltage 100 V and (b) defected niobium oxide nanocolumns formed by anodizing a two-layer Al/Nb system in 0.4 M $C_2H_2O_4$ aqueous solution at a voltage 37 V and reanodized in 0.5 M H_3BO_3 aqueous solution and 0.05 M $Na_2B_4O_7$ to a voltage 190 V. The images show nanostructures after the removal of porous anodic aluminum oxide.

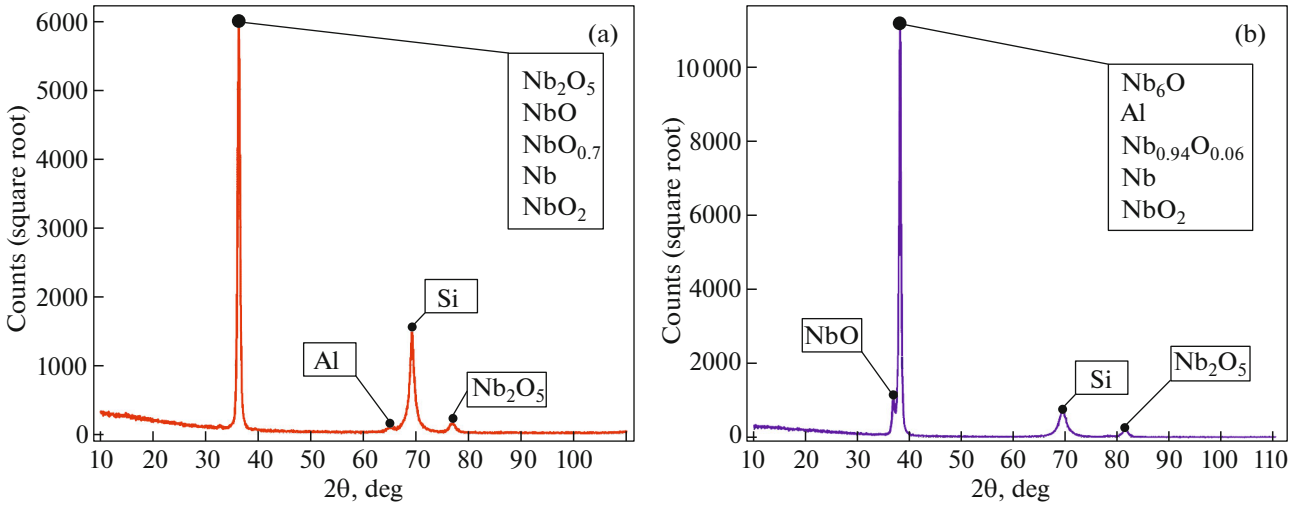

Fig. 3. X-ray phase analysis of (a) defected niobium oxide nonuniform arrays formed by anodizing of a two-layer Al/Nb system in 0.4 M H_3PO_4 aqueous solution at a voltage 100 V and (b) defected niobium oxide nanocolumns formed by anodizing of a two-layer Al/Nb system in 0.4 M $C_2H_2O_4$ aqueous solution at a voltage 37 V and reanodized in 0.5 M H_3BO_3 aqueous solution and 0.05 M $Na_2B_4O_7$ to a voltage 190 V.

can be attributed to highly textured phases NbO, $NbO_{0.7}$, Nb_2O_5. The existence of Nb_2O_5 in NONs was shown earlier in [1, 2]. However, the presence of $NbO_{0.7}$ and NbO oxides in the previous work [11], where the NON composition was researched by the XPS method, was not detected. In addition to these phases associated with strong peaks on diffractograms, the NON contains weakly textured phases in small quantities: NbO_2, Nb_4O_5, and Al. The presence of Al may be due to its incomplete removal after chemical dissolution of the porous AAO, as well as its presence in the NON top. As previously shown [2], the ingress of aluminum into the NON tops occurs during high-voltage reanodizing, when the outer rarefied contaminated layer of the AAO pore is mixed with a niobium anodic oxide that fills the pore. However, as it can be assumed from the results presented, aluminum appears with a high degree of probability in the NON tops and at the anodizing stage. The presence of NbO_2 in the NON spectrum is also quite typical, as was also shown earlier [2]. The continuous oxide layer of nanocolumns that develops from the NON bottom consists entirely of NbO_2. Among these phases, not a large amount of Nb_4O_5 was detected, the presence of which was detected for the first time. As it can be seen from Fig. 2a, defecting process of NON mainly leads to the separation of the NON tops from their bottoms through the stem destruction. And the probable results

of the appearance of new oxide forms on the spectra can morphologically be located only on the breaks of the NON stems.

Figure 3b shows the results of X-ray phase analysis of defected niobium anodic oxide nanocolumns. Before the analysis, the complete removal of the porous AAO was performed. The 36° peak is also on the presented spectrum, but with a lower intensity. This also indicates the probable presence of niobium oxides characteristic of NON: NbO, Nb_2O_5, $NbO_{0.7}$, NbO_2, but in smaller quantities. This results in a strong peak at 38°–39°. It can be associated with $Nb_{0.94}O_{0.06}$, Nb_6O, which is typical for reanodized nanostructures, as shown in [2, 10]. Due to the fact that the column top is hypertrophied and has an elongated shape, defected in process, its destruction may occur in any part, not only at the bottom, as for NON, so it is not possible to conclude unequivocally that the appearance of new oxides is due to their presence in the stems or in the hypertrophied tops.

CONCLUSIONS

Summing up, we can draw the following conclusions. The composition and morphology of defected niobium oxide nonuniform (NON) arrays formed by anodizing differ significantly in morphology and composition from the columns of niobium oxide that are formed by NON reanodizing. In the first case, there is a significant amount of Nb_2O_5, NbO, and $NbO_{0.7}$, as well as small amounts of NbO_2, which is completely correlated with the literature data. In turn, significant amounts of $Nb_{0.94}O_{0.06}$, Nb_6O and small amounts of NbO, Nb_2O_5, $NbO_{0.7}$, NbO_2 were found in the defected niobium oxide nanocolumns, which is expected to be confirmed by the literature data for reanodized nanostructures.

The obtained data expand the understanding of nanostructured niobium oxides and allow them to be used in the future to build the latest devices for nonlinear optics and nanoelectronics.

ACKNOWLEDGMENTS

The authors express their gratitude to the Organizing Committee of the XXIV International Symposium "Nanophysics and Nanoelectronics" for the opportunity to present the research results. The authors thank Ulyana Turovets from the Belarusian State University of Informatics and Radioelectronics (BSUIR) for her help with computer modeling of the scheme of niobium oxide nonuniform arrays formation and Associate Professor of BSUIR, Alexander Poznyak, for valuable discussions.

FUNDING

The work was supported by the state research program of the Republic of Belarus "Convergence 2020" (task 3.03) and the scientific and technical program of the Union State "Technology-SG" (task 2.3.2.1) using the equipment of the center for collective use "Physics and Technology of Micro- and Nanostructures" at the Institute of Microstructure physics of the Russian Academy of Sciences.

CONFLICT OF INTEREST

The authors state that they have no conflicts of interest.

REFERENCES

1. V. Surganov and G. Gorokh, *Symp. on Design, Test, Integration, and Packaging of MEMS/MOEM*, Vol. 4019 (2000). https://doi.org/10.1117/12.382321
2. A. Mozalev, R. M. Vázquez, C. Bittencourt, D. Cossement, F. Gispert-Guirado, E. Liobel, and H. Habazaki, J. Mater. Chem. C **2** (24), 4847 (2014). https://doi.org/10.1039/c4tc00349g
3. A. Pligovka, A. Lazavenka, and A. Zakhlebayeva, *Proc. 18th Int. Conf. Nanotechnology (IEEE-NANO)* (Cork, Ireland, 2018). https://doi.org/10.1109/NANO.2018.8626387
4. A. Pligovka, A. Zakhlebayeva, and A. Lazavenka, J. Phys.: Conf. Ser. **987** (1), 012006 (2018). https://doi.org/10.1088/1742-6596/987/1/012006
5. A. N. Pligovka and G. G. Gorokh, *Nanostructures in Condensed Media: Collection of Scientific Articles* (ITMO im. A. V. Lykova, Minsk, 2014), pp. 310–319 [in Russian].
6. A. Pligovka, A. Lazavenka, and G. Gorokh, IEEE Trans. Nanotechnol. **18** (125), 790 (2019). https://doi.org/10.1109/TNANO.2019.2930901
7. A. Mozalev, A. J. Smith, S. Borodin, A. Plihauka, A. W. Hassel, M. Sakairi, and H. Takahashi, Electrochim. Acta **54** (3), 935 (2009). https://doi.org/10.1016/j.electacta.2008.08.030
8. A. Mozalev, M. Bendova, F. Gispert-Guirado, and E. Llobet, Chem. Mater. **30** (8), 2694 (2018). https://doi.org/10.1021/acs.chemmater.8b00188
9. A. Mozalev, V. Khatko, C. Bittencourt, A. W. Hassel, G. Gorokh, E. Liobel, and X. Correig, Chem. Mater. **20** (20), 6482 (2008). https://doi.org/10.1021/cm801481z
10. G. G. Gorokh, A. N. Pligovka, and A. A. Lozovenko, Tech. Phys. **64** (11), 1657 (2019). https://doi.org/10.1134/S1063784219110124
11. A. Mozalev, M. Sakairi, I. Saeki, and H. Takahashi, Electrochim. Acta **48** (20), 3155 (2003). https://doi.org/10.1016/S0013-4686(03)00345-1
12. M. A. Porai-Koshits, *Fundamentals of Structural Analysis of Chemical Compounds: Textbook* (Vysshaya Shkola, Moscow, 1989) [in Russian].
13. Ya. S. Umansky and N. V. Chirikov, *Physical Encyclopedia* (Great Russian Encyclopedia, Moscow, 1994), Vol. 4, pp. 377–378 [in Russian].

14. V. D. Krylov, *Chemical Encyclopedia* (Great Russian Encyclopedia, Moscow, 1995), Vol. 4, pp. 242–243 [in Russian].
15. V. S. Gorshkov, V. V. Timashev, and V. G. Savel'ev, *Methods for Physicochemical Analysis of Binding Agents: Textbook* (Vysshaya Shkola, Moscow, 1981), p. 335 [in Russian].
16. I. M. Zharskii and G. I. Novikov, *Physical Research Methods in Inorganic Chemistry* (Vysshaya Shkola, Moscow, 1988), p. 271 [in Russian].
17. R. S. Saifullin, *Physicochemistry of Inorganic Polymer and Composite Materials* (Khimiya, Moscow, 1990), p. 240 [in Russian].
18. N. M. Bobkova, *Physical Chemistry of Refractory Nonmetallic and Silicate Materials* (Vysshaya Shkola, Minsk, 2007), p. 301 [in Russian].
19. A. V. Kolpakov, *Physical Encyclopedia* (Sov. Encyclopedia, Moscow, 1988), Vol. 1, pp. 671–674 [in Russian].